COMMUNICATIONS IN SCIENCE AND TECHNOLOGY
Homepage: cst.kipmi.or.id

Microwave-assisted biosynthesis and characterization of ZnO film for photocatalytic application in methylene blue degradation

Ari Sulistyo Rini*, Averin Nabilla, Yolanda Rati

Physics, Faculty of Mathematics and Natural Sciences, Universitas Riau, Pekanbaru 28293, Indonesia

Article history:
Received: 25 July 2021 / Received in revised form: 19 November 2021 / Accepted: 24 November 2021

Abstract

This study aims to investigate the physical characteristics and photocatalyst activity of biosynthesized ZnO with pineapple (*Ananas comosus)* peel extract under microwave irradiation. The ZnO powder was prepared in two different concentrations of zinc nitrate hexahydrate (ZNH) at 200mM (Z-200) and 500 mM (Z-500). The optical, structural, and morphological properties of ZnO were analyzed using UV-Vis spectroscopy, X-Ray Diffraction (XRD), and Scanning Electron Microscopy (SEM), respectively. The UV-Vis absorption spectrum showed a wide absorbance peak of ZnO at the wavelength of 300-360 nm with a bandgap energy of 3.22 and 3.25 eV. The XRD result confirmed the wurtzite structure of ZnO with high crystallinity. SEM morphology showed spherical particles with an average particle size of 190-220 nm. For photocatalytic application, ZnO film was fabricated via the doctor blade method from microwave-assisted biosynthesized ZnO powder. ZnO films were then applied under UV-irradiation to examine the photocatalytic degradation of methylene blue. It was found that the catalytic behavior of ZnO film was affected by the starting ZNH concentration with maximum effectiveness of 46% degradation after 2 h.

Keywords: Zinc oxide; microwave-assisted; photocatalytic activity; methylene blue

1. Introduction

Synthetic dyes containing organic compounds have been frequently used in the textiles, paper, printing, food, and cosmetics industries to make their products. They are difficult to decompose and may cause environmental problems [1]. Methylene blue (MB) dye is one of the liquid wastes that are most commonly found. This material can irritate the digestive tract if swallowed, cause cyanosis if inhaled, and irritate the skin if touched [2]. Here, photodegradation, which obeys the principle of the photocatalyst, is an effective method to degrade such synthetic dye. This method has a number of advantages, such as requiring a simple reactor, no secondary pollution left by the degraded organic substances, and able to be reprocessed in an ecofriendly approach [3].

Commonly, the photodegradation uses a number of semiconductor materials such as TiO_2 [4], Fe_2O_3[5], and ZnO[6]. Of these compounds, ZnO's photocatalytic properties have been extensively studied in view of its excellent oxidation capabilities, non-toxicity, chemical stability, and affordability.

There are several methods to synthesize ZnO, for instance chemical, physical and biological methods. However, chemical and physical methods require toxic material usage and high energy consumption [7]. The biosynthetic method can reduce hazardous chemicals in nanoparticle synthesis. It uses natural products such as plants extracts or microorganisms as reducing agents. This method does not require more energy or high pressure, so it is relatively inexpensive, eco-friendly, and able to be massively produced [8]. Plant extracts contain the high level of antioxidant which can reduce and stabilize nanoparticles. Watermelon peel extract [9], lemon peel extract [10], and sea buckthorn fruit [11] have been used as ZnO bioreductor and bio-stabilizers.

Pineapple is one of the main agricultural commodities in Riau Province, Indonesia. The peels of this plant are frequently discarded without being used. In fact, they can be applied either as the carbon source for chemical adsorbent [12] or as bio-stabilizer in nanoparticle synthesis [13]. Using conventional heating, pineapple peels have successfully produced ZnO nanoparticles [13]. Conventional heating, however, has some problems such as regarding inhomogeneity, which leads to poor crystallization and time consuming [14]. Microwave irradiation heating can overcome this problem due to its short reaction time, less excessive energy consumption, and excellent synthesis products [15].

In this study, the ZnO powder was prepared using pineapple peel extract (PPE) as bio-stabilizing agent with two different precursor concentrations via the microwave irradiation technique. The UV-Vis absorption, bandgap energy, morphology, crystal structure, and photocatalytic activity were then analyzed. The doctor blade technique was used to prepare

* Corresponding author. Tel.: +62-812-7046-4974; fax: +62-761-63273.
Email: ari.sulistyo@lecturer.unri.ac.id
https://doi.org/10.21924/cst.6.2.2021.484

ZnO film for photocatalytic application. The photocatalytic activities of ZnO films were evaluated through the MB degradation process initiated by UV-C light irradiation.

2. Materials and Methods

2.1. Materials

The materials used in this study were $Zn(NO_3)2{\cdot}6H_2O$ (zinc nitrate hexahydrate), Pineapple Peel Extract (PPE), NaOH (Sodium Hydroxide), Polyethylene Glycol (PEG), (C_2H_5OH) ethanol, $C_{16}H_{18}ClN_3S$ (Methylene Blue), and demineralized water (Aqua DM).

2.2. Preparation of ZnO powder and ZnO film

ZnO was prepared by reacting 50 mL of pineapple peel extract (10g/L) and 50 mL of zinc nitrate hexahydrate solution (200 mM and 500 mM) in an Erlenmeyer flask. The solution pH was adjusted to pH level of 11 using NaOH 0.1 M. The synthesis solution was subsequently irradiated using a microwave oven with a power of 360 W for 2 min. Once irradiated, the solution was taken out from the oven and cooled at room temperature. The ZnO powder was then separated by centrifugation and dried at 60℃ for 12 h.

For photocatalytic application, ZnO film was prepared via the doctor blade method in which 1 g of ZnO powder was mixed with 0.1 mL of Polyethylene Glycol (PEG) and 2.5 mL of ethanol to obtain a ZnO paste [16]. The paste was then deposited on a 1 cm x 1.5 cm glass slide. Afterward, the ZnO film was dried at 100℃ and annealed at 275℃ for 1 h.

2.3 Characterization

The optical, structural, and morphological properties of ZnO were characterized using a Cary 60 spectrophotometer with the wavelength range of 300-600 nm, Rigaku MiniFlex diffractometer using CuKα radiation (1.541 Å), and Hitachi Flexsem 1000 at a magnification of up to 20,000 times, respectively.

2.4 Photocatalytic activity study

The photocatalytic activity of ZnO film was examined for MB photodegradation under UV-C light irradiation (253.7 nm). The ZnO film was previously immersed in 1 ppm MB solution and left in the dark for 1 hour until achieving the adsorption-desorption equilibrium. The MB solution was then irradiated using a UV lamp of 40 W. Before irradiation, 3 ml of solution were taken out as the control. After the irradiation process started, the same amount of solution was taken out in every 30 minutes for quantitative analysis. A Cary 60 spectrophotometer was used to monitor the residue concentration of MB. MB concentration reduction was evaluated from the characteristic absorbance peak of MB at 664 nm. The degradation reaction rate and photodegradation efficiency were calculated by the formula (1) and (2), respectively:

$$ln\frac{A}{A_0} = -kt \qquad (1)$$

$$\%D = \frac{A_0 - A}{A_0} \times 100\% \qquad (2)$$

where A is the absorbance of the dye after treatment, A_0 is the absorbance of the initial dye, k is the reaction rate constant, and t is the time[17].

3. Results and Discussion

3.1. UV-Vis absorption properties

Figure 1 shows the UV-Vis absorbance spectrum of ZnO samples. The higher ZNH concentration resulted in an improvement in the absorption ability of the ZnO sample. The optical properties of the sample showed a ZnO typical broad absorbance in the wavelength range of 300-360 nm and at 360-600 nm.

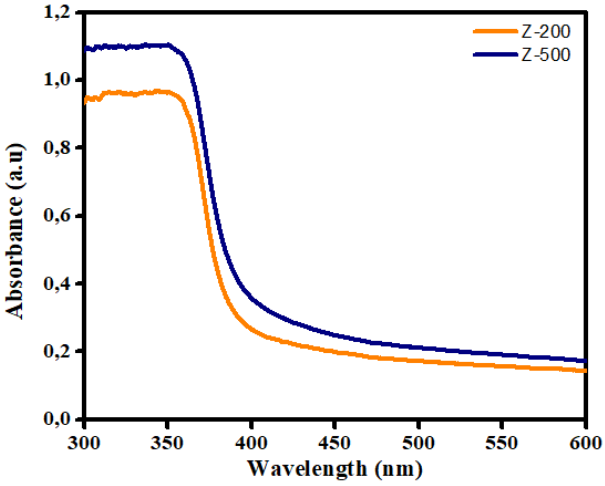

Fig. 1. UV-Vis absorbance spectrum of ZnO

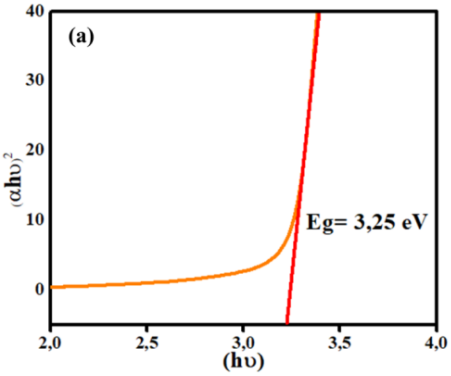

(a)

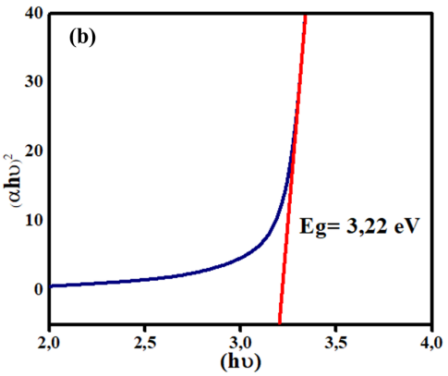

(b)

Fig. 2. Bandgap energy (a) (hυ) vs $(\alpha h\upsilon)^2$ Z-200 dan (b) Z-500

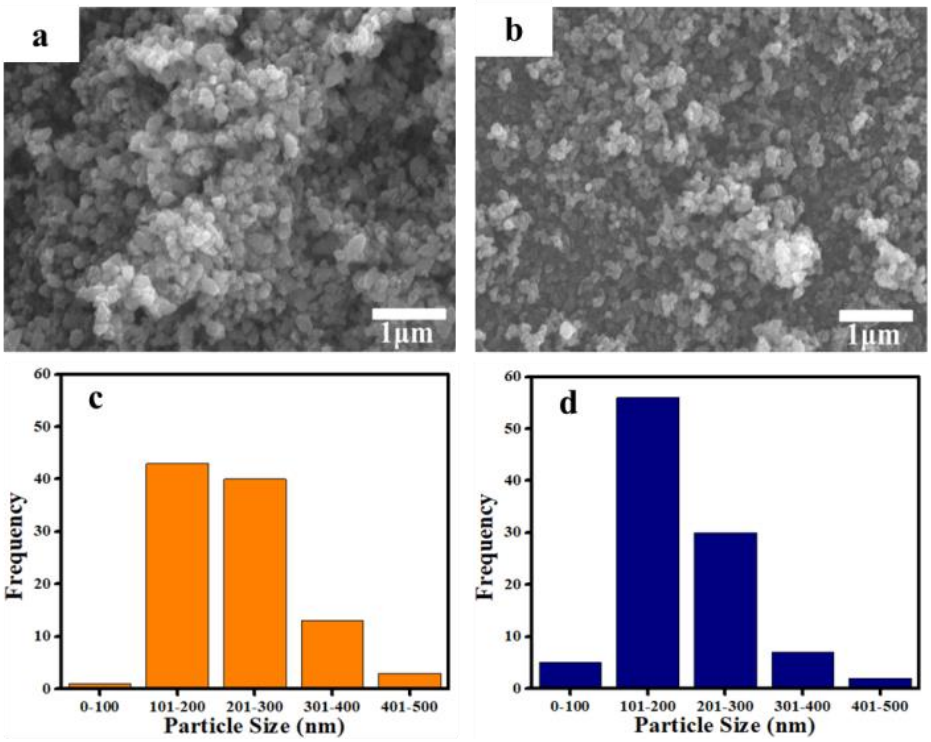

Fig. 3. SEM Images and histogram diagram of ZnO (a,c) Z-200 and (b,d) Z-500

It also showed that the increasing concentration of Zinc nitrate could cause the widening ZnO maximum absorbance at the wavelength from 360 nm (sample Z-200) to 380 nm (Z-500). The shift in the absorbance peak was most probably attributed to the increase in particle size [18].

Optical absorption indicated the minimum photon energy required for electrons to be excited from the valence band to the conduction band [19]. The bandgap energy of the ZnO sample was obtained from the Tauc plot equation through the intersection of the line between ($h\upsilon$) vs $(\alpha h\upsilon)^2$. The bandgap energy of samples Z-200 and Z-500 included 3.25 eV and 3.22 eV, respectively. The Z-500 sample had the lower bandgap energy compared to the Z-200. This was because the high light absorption had caused the energy bandgap of the material to decrease [20]. The bandgap energy obtained from the biosynthesis method was found less compared to the bandgap energy of ZnO using the chemical method (precipitation), i.e. 3.38 eV [21]. The bandgap energy value was also determined by particle size, carrier concentration, stress state in the material, and oxygen vacancies, later on affecting the carrier concentration in the conduction band [22].

3.2 Morphological analysis

The particle size of the Z-200 sample is in the range of 221.57 ± 73.93 nm, while the one in Z-500 sample is 194.87 ± 75.52 nm. The higher the concentration of Zinc nitrate, the smaller the particle size. In addition, higher Zinc nitrate concentration produce more uniform (homogeneous) particles. The uniformity of particle size is known from the standard deviation value. It is because, during the microwave irradiation process, high concentrations will accelerate the reaction rate that reduces the particle size [23]. The smaller particle size is also due to the presence of phenolic compounds contained in PPE, which act not only as a stabilizing agent but also as a reducing agent [18].

Figure 3 shows the SEM image of the ZnO sample using PPE with a magnification of 20,000 times. The morphology of the ZnO sample is spherical. This morphology is similar to ZnO film synthesized using watermelon rind extract [9].

3.3 Crystal structure

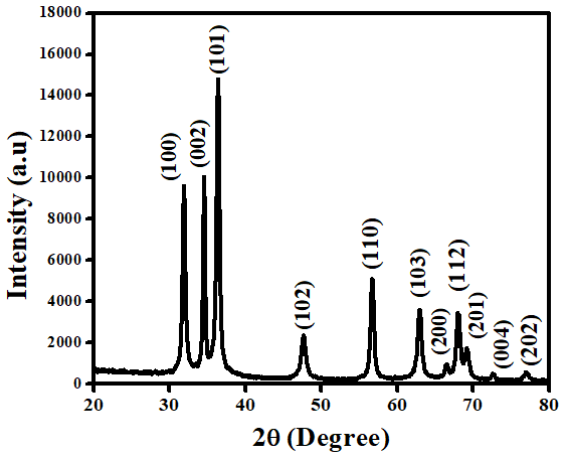

Fig. 4. XRD pattern of ZnO

Figure 4 shows the X-ray diffraction pattern of ZnO sample. The diffraction peaks were at the Bragg angle of 2Θ = 31,84˚; 34,50 ˚; 36,35˚; 47,63˚ ; 56,77˚; 63,03˚; 66,40˚; 67,96˚; 69,2˚; 72,67˚; 76,89˚ which corresponded to ZnO wurtzite hkl plane of (100), (002), (101), (102), (110), (103), (200), (112), (201), (004), (202), respectively[24]. Sharp diffraction peaks with high intensity indicated the high crystallinity of ZnO. In addition, there were no impurities in the ZnO sample evidenced

by no diffraction peaks other than the ZnO phase. The crystal size was measured using the Scherrer formula:

$$D(nm) = \frac{k\lambda}{\beta cos\theta} \quad (3)$$

For a hexagonal structure, the lattice parameters a and c were

$$\frac{1}{d^2} = \frac{4h^2+hk+k^2}{a^2} = \left(\frac{1}{c^2}\right) \quad (4)$$

where D is the crystal size, β is the width of half the maximum diffraction peak (FWHM), λ is the wavelength, k is a constant whose value varies, and θ is the diffraction angle. The FWHM value was 0.0078˚ so that the crystal size obtained was 17.55 nm. The calculated values of the lattice constants of the ZnO particles included a = b = 3.1173 Å and c = 5.1931 Å.

3.4 Photocatalytic activity

Figure 5 shows the absorption spectrum of MB solution sampled in every 30 min. It represents the photodegradation of MB by ZnO sample from time to time. Photodegradation using Z-200 and Z-500 samples showed a change in the colour of MB and became clear at 120 minutes, especially the Z-200 sample. This color change was quantitatively analyzed from the methylene blue absorption peak.

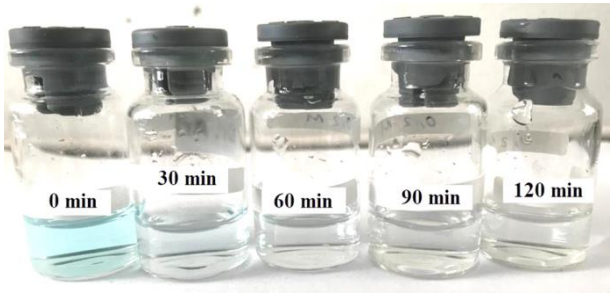

(a)

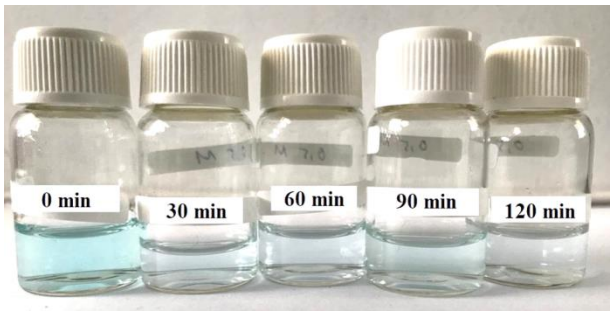

(b)

Fig. 5. The degradation process of MB by (a) Z-200 and (b) Z-500 samples

Figure 6(a) is the curve of absorption of degradation product of ZnO sample at λ = 662 nm versus time. The degradation of MB occurred on the ZnO surface. This reduction process was attributed to the hydroxyl radical OH^- from the oxidation of water and the oxygen, which prevented the recombination of electron-hole pairs[25]. Figure 6(b) shows the $ln\, A/A_0$ vs. time curve indicating the photocatalytic degradation rate of MB dye where ZnO acted as a catalyst. Z-200 sample had a reaction rate constant of 0.1552 min^{-1} greater than that of Z-500 i.e. 0.1114 min^{-1}. Z-200 sample had a higher reaction rate because the sample had a large bandgap energy value to prevent the charge recombination. The reaction rate constant implied an increase in the number of dye molecules and a reduction of photon path length so that fewer photons reached the catalyst surface. It may cause a decrease in the generation of hydroxyl radicals and reactive superoxides [19].

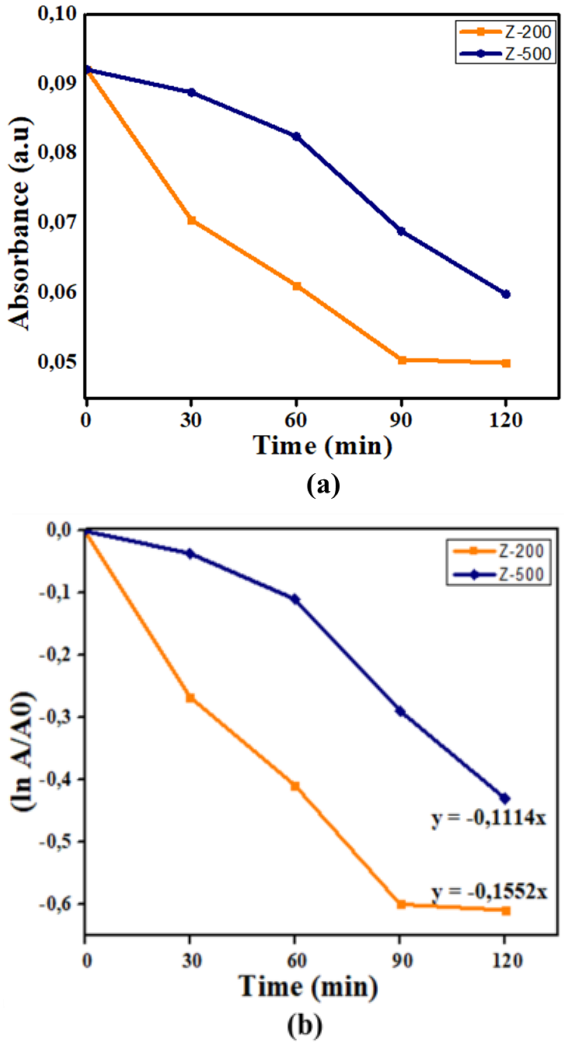

Fig. 6. (a) Absorption curve of MB at λ = 662 nm (b) Graph of ln A/A0 versus degradation time

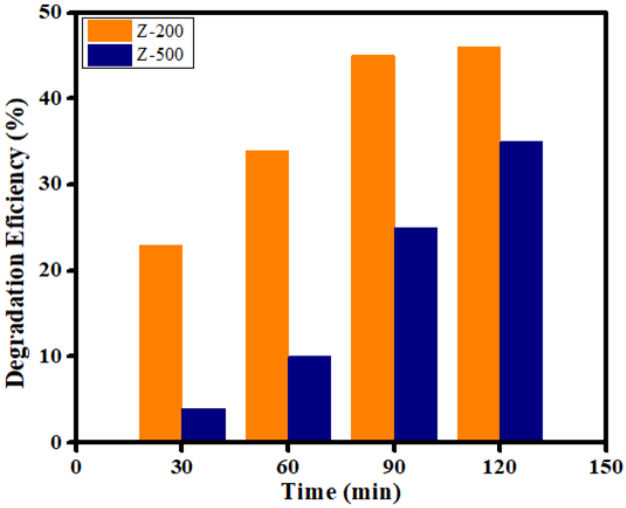

Fig 7. Percentage of degradation of MB dye after 120 minutes of irradiation

The degradation efficiency of the Z-200 and Z-500 samples after 120 min was 46% and 35%, respectively (Figure 7). Photocatalyst activity was closely related to particle size, where decreasing particle size could increase the surface area where the photodegradation took place. The photodegradation efficiency was also improved by increasing the bandgap energy [26]. Therefore, Z-200 and Z-500 samples with particle sizes of 221.57 nm and 194.87 nm, respectively, were effective in degrading MB dye.

Conclusion

In this research, the ZnO sample has been successfully synthesized using pineapple peel extract via the microwave irradiation method. It was found that the concentration affected the UV-Vis absorption peak and the ZnO particle size of ZnO samples. Biosynthesized ZnO assisted by MW exhibited high purity and crystallinity. The photocatalytic activity test showed that ZnO film prepared from biosynthesis product was effective in the degradation of MB dye. ZnO sample can be potentially used as a photocatalyst material for wastewater treatment applications.

References

1. K. A. Isai and V. S. Shrivastava, *Photocatalytic degradation of methylene blue using ZnO and 2%Fe–ZnO semiconductor nanomaterials synthesized by sol–gel method: a comparative study*, J. Water Environ. Nanotechnol., 4(3) (2019) 251–262.
2. K. Murali and R. N. Uma, Removal of Basic Dye (Methylene Blue) Using Low Cost Biosorbent : Water Hyacinth, Int. Adv. Eng. Technol. 7 (2016) 386-391.
3. S. Kumar, W. Ahlawat, G. Bhanjana, S. Heydarifard, M. M. Nazhad, and N. Dilbaghi, "*Nanotechnology-based water treatment strategies*, J. Nanosci. Nanotechnol. 14 (2014) 1838–1858.
4. A. Jain and D. Vaya, *Photocatalytic Activity of TiO_2 Nanomaterial*, J. Chil. Chem. Soc. 62 (2017) 3661–3668.
5. Y. Q. Cao, et al., *Enhanced visible light photocatalytic activity of Fe_2O_3 modified TiO_2 prepared by atomic layer deposition*, Sci. Rep.10 (2020) 1–10.
6. S. Bhatia and N. Verma, *Photocatalytic activity of ZnO nanoparticles with optimization of defect*s, Mater. Res. Bull. 95 (2017) 468–476.
7. Z. Muslim, K. Aadim, and R. Kadhim, *Preparation of ZnO for Photocatalytic Activity of Methylene Blue Dye*, Int. J. Basic Appl. Sci. 6 (2017) 1–7.
8. S. M. Tabrizi Hafez Moghaddas, B. Elahi, and V. Javanbakht, *Biosynthesis of pure zinc oxide nanoparticles using Quince seed mucilage for photocatalytic dye degradation*, J. Alloys Compd. 821 (2020) 1-9.
9. A.S. Rini, S. D. Rahayu, Y. Hamzah, T. M. Linda and Y. Rati, *Effect of pH on the Morphology and Microstructure of ZnO synthesized using Ananas Comosus Peel Extract*, J. Phys. Conf. Ser. 2019 (2021) 1-7.
10. O. J. Nava *et al.*, *Fruit peel extract mediated green synthesis of zinc oxide nanoparticles*, J. Mol. Struct. 1147 (2017) 1–6.
11. E. J. Rupa, L. Kaliraj, S. Abid, D. C. Yang, and S. K. Jung, *Synthesis of a zinc oxide nanoflower photocatalyst from sea buckthorn fruit for degradation of industrial dyes in wastewater treatment*, Nanomaterials. 9 (2019) 1–18.
12. A. Bayu *et al.*, I*sotherm adsorption characteristics of carbon microparticles prepared from pineapple peel waste*, Commun. Sci. Technol. 5 (2020) 31–39.
13. H. H. Basri, R. A. Talib, R. Sukor, S. H. Othman, and H. Ariffin, *Effect of synthesis temperature on the size of ZnO nanoparticles derived from pineapple peel extract and antibacterial activity of ZnO–starch nanocomposite films*, Nanomaterials. 10 (2020) 1-15.
14. B. G. Rao, D. Mukherjee, and B. M. Reddy, *Novel approaches for preparation of nanoparticles*. Elsevier Inc., 2017 1-31.
15. A. S. Rini, S. Radiman, and M. A. Yarmo, *Microwave-assisted Synthesis of Ru-Sn/ZnO for Catalysis Application,* AIP Conf. Proc. 1284 (2010) 129–133.
16. A. Al-Kahlout, *Thermal treatment optimization of ZnO nanoparticles-photoelectrodes for high photovoltaic performance of dye-sensitized solar cells*, J. Assoc. Arab Univ. Basic Appl. Sci. 17 (2015) 66–72.
17. G. Verma and M. Mishra, *Development and Optimization of Uv-Vis Spectroscopy-a Review*, World J. Pharm. Res.7 (2018) 1170–1180.
18. M. J. Haque, M. M. Bellah, M. R. Hassan, and S. Rahman, *Synthesis of ZnO nanoparticles by two different methods & comparison of their structural, antibacterial, photocatalytic and optical properties*, Nano Express. 1 (2020) 1-13.
19. N. Rana, S. Chand, and A. K. Gathania, *Green synthesis of zinc oxide nano-sized spherical particles using Terminalia chebula fruits extract for their photocatalytic applications*, Int. Nano Lett., 6 (2016) 91–98.
20. A. Fuad, A. A. Fibriyanti, Subakti, N. Mufti, and A. Taufiq, *Effect of Precursor Concentration Ratio on the Crystal Structure, Morphology, and Band Gap of ZnO Nanorods*, *I*OP Conf. Ser. Mater. Sci. Eng. 202 (2017) 1-8.
21. M. J. Chithra, M. Sathya, and K. Pushpanathan, *Effect of pH on crystal size and photoluminescence property of zno nanoparticles prepared by chemical precipitation method*, Acta Metall. Sin. English Lett. 28 (2015) 394–404.
22. A. F. Abdulrahman, S. M. Ahmed, and M. A. Almessiere, *Effect of the growth time on the optical properties of ZnO nanorods grown by low temperature method*, Dig. J. Nanomater. Biostructures. 12 (2017) 1001–1009.
23. K. R. Ahammed *et al*., *Microwave assisted synthesis of zinc oxide (ZnO) nanoparticles in a noble approach: utilization for antibacterial and photocatalytic activity*, SN Appl. Sci. 2 (2020) 1–14.
24. A. S. Rini, Y. Rati, A. A. Umar, and N. A. Abdullah, *Investigation of structural, morphological and optical properties of sulfur doped zinc oxide nanorod*, Int. J. Nanoelectron. Mater. 13 (2020) 21–32.
25. M. Irani, T. Mohammadi, and S. Mohebbi, *Photocatalytic degradation of methylene blue with zno nanoparticles; a joint experimental and theoretical study*, J. Mex. Chem. Soc. 60 (2016) 218–225.
26. Q. Zhang, M. Xu, B. You, Q. Zhang, H. Yuan, and K. Ostrikov, *Oxygen vacancy-mediated ZnO nanoparticle photocatalyst for degradation of methylene blue*, Appl. Sci. 8 (2018) 1–12.